

Large-System Analysis of Multiuser Detection With an Unknown Number of Users: A High-SNR Approach

Adrià Tauste Campo, *Student Member, IEEE*, Albert Guillén i Fàbregas, *Senior Member, IEEE*, and
Ezio Biglieri, *Life Fellow, IEEE*

Abstract—We analyze multiuser detection under the assumption that the number of users accessing the channel is unknown by the receiver. In this environment, users' activity must be estimated along with any other parameters such as data, power, and location. Our main goal is to determine the performance loss caused by the need for estimating the identities of active users, which are not known *a priori*. To prevent a loss of optimality, we assume that identities and data are estimated jointly, rather than in two separate steps. We examine the performance of multiuser detectors when the number of potential users is large. Statistical-physics methodologies are used to determine the macroscopic performance of the detector in terms of its multiuser efficiency. Special attention is paid to the fixed-point equation whose solution yields the multiuser efficiency of the optimal (maximum *a posteriori*) detector in the large signal-to-noise ratio regime. Our analysis yields closed-form approximate bounds to the minimum mean-squared error in this regime. These illustrate the set of solutions of the fixed-point equation, and their relationship with the maximum system load. Next, we study the maximum load that the detector can support for a given quality of service specified by error probability.

Index Terms—Asymptotic analysis, multiuser detection, multiuser efficiency, statistical physics.

I. INTRODUCTION

IN multiple-access communication, the evolution of user activity may play an important role. From one time instant to the next, some new users may become active and some users inactive, while the parameters of the active users, such as power or location, may vary. Now, most of the available multiuser detection (MUD) theory is based on the assumption that the number of active users is constant, known at the receiver, and equal to the maximum number of users entitled to access the system [1]. If this assumption does not hold, the receiver may exhibit a serious

performance loss [2], [6]. In [7], the more realistic scenario in which the number of active users is unknown *a priori*, and varies with time with known statistics, is the basis of a new approach to detector design. This work presents a large-system analysis of this new type of detectors for code division multiple access (CDMA).

Our main goal is to determine the performance loss caused by the need for estimating the identities of active users, which are not known *a priori*. In this paper we restrict our analysis to a worst-case scenario, where detection cannot improve the performance from past experience due to a degeneration of the activity model (for instance, assuming a Markovian evolution of the number of active users [3], [4]) into an independent process [5]. The same analysis applies to systems where the input symbols accounting for data and activity are interleaved before detection. To prevent a loss of optimality, we assume that identities and data are estimated jointly, rather than in two separate steps. Our interest is in randomly spread CDMA system in terms of multiuser efficiency, whose natural dimensions (number of users K , and spreading gain N) tend to infinity, while their ratio (the “system load”) is kept fixed. In particular, we consider the optimal maximum *a posteriori* (MAP) multiuser detector, and use tools recently adopted from statistical physics [8], [9], [11]–[13], [29]. Of special relevance in our analysis is the decoupling principle introduced in [9] for randomly spread CDMA. The general results derived from asymptotic analysis are validated by simulations run for a limited number of users [12].

The results of this paper focus on the degradation of multiuser efficiency when the uncertainty on the activity of the users grows and the SNR is sufficiently large. We go one step beyond the application of the large-system decoupling principle [8], [9] and provide a new high-SNR analysis on the set of fixed-point solutions showing explicitly its interplay with the system load for a nonuniform ternary and parameter-dependent input distribution. By expanding the minimum mean square error for large SNR, we obtain tight closed-form bounds that describe the large CDMA system as a function of the SNR, the activity factor and the system load. In addition, some tradeoff results between these quantities are derived. Of special novelty here is the study of the impact of the activity factor in the CDMA performance measures (minimum mean-square error, and multiuser efficiency). In particular, we provide necessary and sufficient conditions on the existence of single or multiple fixed-point solutions as a function of the system load and SNR. Finally, we analytically

Manuscript received September 19, 2008; revised May 18, 2010; accepted July 26, 2010. Date of current version May 25, 2011. E. Biglieri was supported by a grant from King Saud University, Riyadh, Saudi Arabia. This work was supported by the Spanish Ministry of Education and Science under Project CONSOLIDER-INGENIO 2010 CSD2008-00010 COMONSENS. The material in this paper was presented in part at the 2009 IEEE Information Theory Workshop, Taormina, Italy, October 2009.

A. Tauste Campo and A. Guillén i Fàbregas are with the Department of Engineering, University of Cambridge, Cambridge CB2 1PZ U.K. (e-mail: atauste@ieee.org; guillen@ieee.org).

E. Biglieri is with the Universitat Pompeu Fabra, c/ Roc Boronat 138, E-08018 Barcelona, Spain, and also with King Saud University, Riyadh, Saudi Arabia (e-mail: ezio.biglieri@upf.edu).

Communicated by A. J. van Wijnngaarden, Associate Editor for Communications.

Digital Object Identifier 10.1109/TIT.2011.2132410

identify the region of “meaningful” multiuser efficiency solutions with their associated maximum system loads, and derive consequences for engineering problems of practical interest.

This paper is organized as follows. Section II introduces the system model and the main notations used throughout. Section III derives the large-system central fixed-point equation, and analytical bounds to the MMSE. Based on these results, Section IV discusses the interplay of maximum system load and multiuser efficiency. Finally, Section V draws some concluding remarks.

II. SYSTEM MODEL

We consider a CDMA system with an unknown number of users [7], and examine the optimum user-and-data detector. In particular, we study randomly spread direct-sequence (DS) CDMA with a maximum of K active users

$$\mathbf{y}_t = \mathbf{S}\mathbf{A}\mathbf{b}_t + \mathbf{z}_t, \quad (1)$$

where $\mathbf{y}_t \in \mathbb{R}^N$ is the received signal at time t , N is the length of the spreading sequences, $\mathbf{S} \in \mathbb{R}^{N \times K}$ is the matrix of the sequences, $\mathbf{A} = \text{diag}(a_1, \dots, a_K) \in \mathbb{R}^{K \times K}$ is the diagonal matrix of the users’ signal amplitudes, $\mathbf{b}_t = (b_t^1, \dots, b_t^K) \in \mathbb{R}^K$ is the users’ data vector, and \mathbf{z}_t is an additive white Gaussian noise vector with i.i.d. entries $\sim \mathcal{N}(0, 1)$. We define the system’s activity rate as $\alpha \triangleq \Pr\{\text{user } k \text{ is active}\}$, $1 \leq k \leq K$. Active users employ binary phase-shift keying (BPSK) with equal probabilities. This scheme is equivalent to one where each user transmits a ternary constellation $\mathcal{X} \triangleq \{-1, 0, +1\}$ with probabilities $\Pr\{b_t^k = -1\} = \Pr\{b_t^k = +1\} = \frac{\alpha}{2}$ and $\Pr\{b_t^k = 0\} = 1 - \alpha$. We define the maximum system load as $\beta \triangleq \frac{K}{N}$.

In a static channel model, the detector operation remains invariant along a data frame, indexed by t , but we often omit this time index for the sake of simplicity. Assuming that the receiver knows \mathbf{S} and \mathbf{A} , the *a posteriori* probability (APP) of the transmitted data has the form

$$p(\mathbf{b} | \mathbf{y}, \mathbf{S}, \mathbf{A}) = \frac{1}{\sqrt{2\pi}} e^{-\frac{\|\mathbf{y} - \mathbf{S}\mathbf{A}\mathbf{b}\|^2}{2}} \frac{p(\mathbf{b})}{p(\mathbf{y} | \mathbf{S}, \mathbf{A})}. \quad (2)$$

Hence, the MAP joint activity-and-data multiuser detector solves

$$\hat{\mathbf{b}} = \arg \max_{\mathbf{b} \in \mathcal{X}^K} p(\mathbf{b} | \mathbf{y}, \mathbf{S}, \mathbf{A}). \quad (3)$$

Similarly, optimum detection of single-user data and activity is obtained by marginalizing over the undesired users as follows:

$$\hat{b}^k = \arg \max_{b^k} \sum_{\mathbf{b} \setminus b^k} p(\mathbf{b} | \mathbf{y}, \mathbf{S}, \mathbf{A}). \quad (4)$$

A. The Decoupling Principle

In a communication scheme such as the one modeled by (2), the goal of the multiuser detector is to infer the information-bearing symbols given the received signal \mathbf{y} and the knowledge about the channel state. This leads naturally to the choice of the partition function $Z(\mathbf{y}, \mathbf{S}) = p(\mathbf{y} | \mathbf{S})$. The corresponding free energy, normalized by the number of users becomes [8]

$$\mathcal{F}_K \triangleq -\frac{1}{K} \ln p(\mathbf{y} | \mathbf{S}). \quad (5)$$

To calculate this expression we make the self-averaging assumption, which states that the randomness of (5) vanishes as $K \rightarrow \infty$. This is tantamount to saying that the free energy per user \mathcal{F}_K converges in probability to its expected value over the distribution of the random variables \mathbf{y} and \mathbf{S} , denoted by

$$\mathcal{F} \triangleq \lim_{K \rightarrow \infty} \mathbb{E} \left\{ -\frac{1}{K} \ln p(\mathbf{y} | \mathbf{S}) \right\}. \quad (6)$$

Evaluation of (6) is made possible by the *replica method* [11], [13], which consists of introducing n independent replicas of the input variables, with corresponding density $p^n(\mathbf{y} | \mathbf{S})$, and computing \mathcal{F} as follows:

$$\mathcal{F} = -\lim_{n \rightarrow 0} \frac{\partial}{\partial n} \left(\lim_{K \rightarrow \infty} \frac{1}{K} \ln \mathbb{E} \{ p^n(\mathbf{y} | \mathbf{S}) \} \right). \quad (7)$$

To compute (7), one of the cornerstones in large deviation theorem, the Varadhan’s theorem [21], is invoked to transform the calculation of the limiting free energy into a simplified optimization problem, whose solutions are assumed to exhibit symmetry among its replicas. More specifically, in the case of a MAP individually optimum detector, the optimization yields a fixed-point equation, whose unknown variable corresponds to the multiuser efficiency of an equivalent Gaussian channel [9]. The multiuser efficiency reflects the degradation factor of SNR due to interference [1]. Due to the structure of the optimization problem, the multiuser efficiency must minimize the free energy. The above is tantamount to formulating the *decoupling principle*.

Claim 2.1: [9], [12] Given a multiuser channel, the distribution of the output b^k of the individually optimum (IO) detector, conditioned on $b^k = b$ being transmitted with amplitude a , converges to the distribution of the posterior mean estimate of the single-user Gaussian channel

$$y = \sqrt{\gamma} b^k + \frac{1}{\sqrt{\eta}} z, \quad (8)$$

where $z \sim \mathcal{N}(0, 1)$, and η , the multiuser efficiency, is the solution of the following fixed-point equation:

$$\eta^{-1} = 1 + \beta \mathbb{E}_\gamma [\gamma \text{MMSE}(\eta\gamma, \alpha)]. \quad (9)$$

If (9) admits more than one solution, we must choose the one that minimizes the free energy function

$$\mathcal{F} = -\mathbb{E} \left[\int p(y | b^k) \ln p(y | b^k) dy \right] - \frac{1}{2} \ln \frac{2\pi e}{\eta} + \frac{1}{2\beta} \left(\eta \ln \frac{2\pi}{\eta} \right). \quad (10)$$

In (9), (10), $p(y | b^k)$ is the transition probability of the large-system equivalent single-user Gaussian channel described by (8), and

$$\text{MMSE}(\eta\gamma, \alpha) \triangleq \mathbb{E} \left[(b^k - \hat{b}^k)^2 \right] \quad (11)$$

denotes the minimum mean-square error in estimating b^k in Gaussian noise with amplitude equal to $\sqrt{\gamma}$, where $\hat{b}^k = \mathbb{E}[b^k | y]$ is the posterior mean estimate, which is known to minimize the MMSE [22].

B. A Note on the Validity of the Replica Method

The replica method is known to accurately approximate experimental data and is consistent with previous theoretical work [19], [23], [24]. The replica method analysis relies on four unproved assumptions: i) the self-averaging property of the free energy; ii) the replica symmetry of the fixed-point solutions; iii) the exchange of order of limits; and iv) the analytic continuation of the replica exponent to real values. Although the validation of the mathematical rigor of these assumptions is still an unsolved problem, there has been some recent progress in this direction [14], [25]–[28].

III. LARGE-SYSTEM MULTIUSER EFFICIENCY

We illustrate here the behavior of multiuser efficiency and system load in the high-SNR region corresponding to detection with an unknown number of users. We start by shaping our problem into the statistical-physics framework [8], [9]. As mentioned earlier, the multiuser detector metric is regarded as the energy of a system of particles at state \mathbf{X} . Therefore, the partition function $Z(\mathbf{X}) = \sum_{\mathbf{x}} \exp(-\varepsilon(\mathbf{x})/T)$ corresponds to the output density given the channel information, i.e., $p(\mathbf{y} | \mathbf{S}) = (2\pi)^{-1/2} \sum_{\mathbf{b}} p(\mathbf{b}) \exp(-\|\mathbf{y} - \mathbf{S}\mathbf{A}\mathbf{b}\|^2/2)$.

The energy operator $\varepsilon(\cdot)$, as derived from the free energy, is related to the logarithm of the joint distribution $p(\mathbf{y} | \mathbf{b}, \mathbf{S})p(\mathbf{b})$

$$\varepsilon(\mathbf{b}) = \|\mathbf{y} - \mathbf{S}\mathbf{A}\mathbf{b}\|^2 - 2 \ln p(\mathbf{b}). \quad (12)$$

We can now invoke the decoupling principle (Claim 2.1) in the multiuser system (1), so as to use its single-user characterization. By doing this, the system's performance can be characterized by that of a bank of K scalar Gaussian channels (8), where K represents the maximum number of users. The input distribution for an arbitrary BPSK user k takes values $\mathcal{X} = \{-1, 0, +1\}$ with probabilities $\frac{\alpha}{2}$, $1 - \alpha$ and $\frac{\alpha}{2}$, respectively. The signal amplitudes from matrix \mathbf{A} are assumed to be constant, i.e., $a_k = \sqrt{\gamma} \forall k$, where γ is the SNR per active user (referred to as SNR), and the inverse noise variance is equal to the multiuser efficiency η . Hence, η is the solution of the fixed-point (9) that minimizes (10), where the MMSE is given by (11). More generally, the analysis presented in this paper can be easily extended to a_k coefficients with different statistics, like for example those induced by Rayleigh fading.

By applying [9, Claim 2.1], which holds under the assumptions of the replica method, the fixed-point equation of the user-and-data detector can be stated as follows.

Corollary 3.1: Given a randomly spread DS-CDMA system with constant equal power per user, the large-system multiuser efficiency of an individually optimum detector that performs MAP estimation of users' identities and their data under BPSK transmission is the solution of the following fixed-point equation:

$$\eta = \frac{1}{1 + \beta \left(\gamma \left[\alpha - \int \frac{1}{\sqrt{2\pi}} e^{-\frac{y^2}{2}} \frac{\alpha^2 \sinh(\eta\gamma - y\sqrt{\eta\gamma})}{\alpha \cosh(\eta\gamma - y\sqrt{\eta\gamma}) + (1-\alpha)e^{\frac{y}{\sqrt{\eta\gamma}}}} dy \right] \right)} \quad (13)$$

that minimizes the free energy (10).

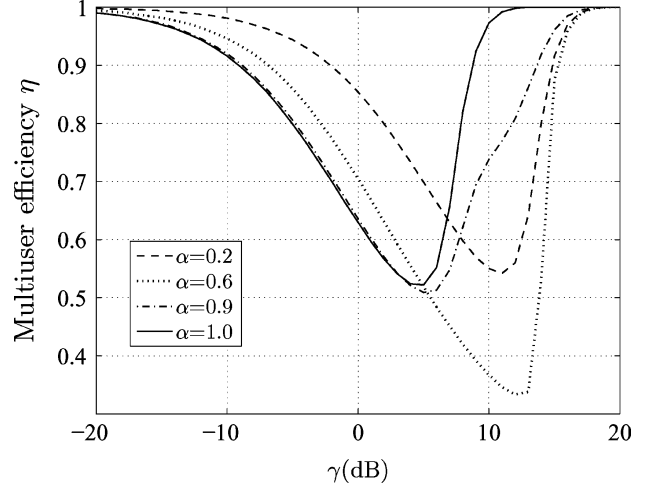


Fig. 1. Large-system multiuser efficiency of the user-and-data detector under MAP with prior knowledge of α and $\beta = 3/7$.

Proof: See Appendix I. ■

Our approach differs from that in [8], [9], and [20], as the fixed-point equation (13) also includes the prior distribution on the users' activity in a static channel. Under MAP estimation, detection requires the knowledge not only of the prior information of the data, but also of the activity rate α . Thus, the solutions to the fixed-point equation depend on the MMSE, SNR, and system load. Numerical solutions versus SNR at a load $\beta = 3/7$ are shown in Fig. 1. Plots like this one illustrate how the multiuser efficiency is affected by the level of noise and interference, and by the uncertainty in the users' activity rate. For low SNR, noise dominates, and the performance of the MMSE and the multiuser efficiency is degraded as α grows, since the presence of more active users adds more noise to the system. On the other hand, as we shall discuss later, for high SNR the MMSE strongly depends on the minimum distance between the transmitted symbols, and the activity rate here plays a secondary role. Hence, the gap between the multiuser efficiencies with $\alpha = 1$ and $\alpha \neq 1$ for larger SNR is due to the fact that the former constellation has twice the minimum distance of the latter. We can observe clearly the transition behavior from low to high SNR for values of α approaching 1. Moreover, when $\alpha = 1$, (13) reduces to the fixed-point equation for the classical assumption, in which all users are active and transmit a binary antipodal constellation [9]

$$\eta^{-1} = 1 + \beta \left(\gamma \left[1 - \int \frac{1}{\sqrt{2\pi}} e^{-y^2/2} \tanh(\eta\gamma - y\sqrt{\eta\gamma}) dy \right] \right). \quad (14)$$

In this case, it can be shown that, for high SNR, we have $\text{MMSE}(\eta\gamma, \alpha = 1) \approx \sqrt{\frac{2\pi}{\eta\gamma}} e^{-\eta\gamma/2}$. In fact, the following general result holds.

Lemma 3.2: [30] For large output SNR, the MMSE of a system transmitting an equiprobable M -ary normalized constellation with minimum Euclidean distance d in a Gaussian channel with noise variance $1/\eta$ is

$$\text{MMSE}(\eta\gamma, \alpha = 1) = \kappa(\eta\gamma) e^{-d^2 \eta\gamma/8} \quad (15)$$

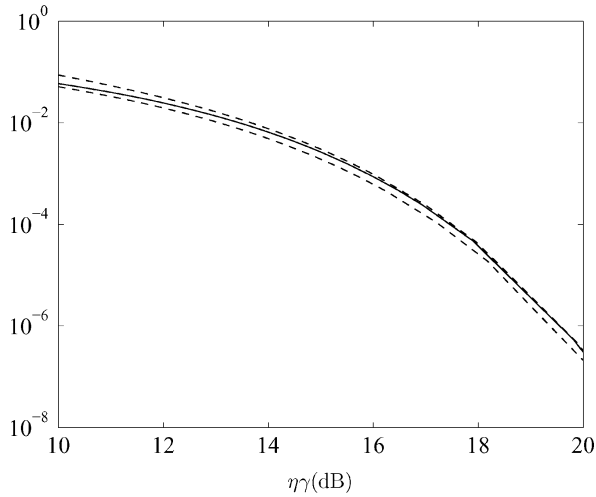


Fig. 2. A comparison of the exact MMSE value with its upper and lower bounds for $\alpha = 0.5$ and $\eta\gamma \in [10, 20]$ dB.

with $\kappa_1(\eta\gamma) \leq \kappa(\eta\gamma) \leq \kappa_2$, where $\kappa_1(\eta\gamma) = \mathcal{O}(1/\sqrt{\eta\gamma})$ and κ_2 is a constant, given by the maximum distance between neighboring symbols.

For the entire range of activity rates, i.e., $\alpha \in [0, 1]$, we can derive lower and upper bounds illustrating analytically the transition between the classical assumption ($\alpha = 1$) and the cases where the activity is also detected ($\alpha < 1$) for large SNR. Our calculations bring about a new analytical framework to deal with large-system analysis, as we will see in the next section. Our bounds are consistent with Lemma 3.2 and the lower bound includes the case $\alpha = 1$. The general result is stated as follows.

Theorem 3.3: The MMSE of joint user identification and data detection in a large system with an unknown number of users has the following behavior, valid for sufficiently large values of the product $\eta\gamma$

$$\begin{aligned} \text{MMSE}(\eta\gamma, \alpha) &\geq 2\sqrt{\frac{\alpha(1-\alpha)}{\pi\eta\gamma}}e^{-\eta\gamma/8} \\ \text{MMSE}(\eta\gamma, \alpha) &\leq 2\alpha e^{-\eta\gamma/2} + \sqrt{\frac{\pi\alpha(1-\alpha)}{\eta\gamma}}e^{-\eta\gamma/8}. \end{aligned} \quad (16)$$

Proof: See Appendix II. ■

Bounds in (16) describe explicitly, in the high-SNR region, the relationship between the MMSE, the users' activity rate, and the effective SNR ($\eta\gamma$). In Fig. 2 these bounds are compared to the true MMSE values as a function of $\eta\gamma$ for fixed α . It can be seen that the uncertainty about the users' activity modifies substantially the exponential decay of the MMSE for high SNR. In fact, a value of α different from 1 causes the MMSE to decay by $\exp(-\eta\gamma/8)$, rather than by $\exp(-\eta\gamma/2)$, which would be the case when all users are active. Furthermore, we can observe that, for sufficiently large effective SNR, the behavior versus α of the optimal detector is symmetric with respect to $\alpha = 1/2$, which corresponds to the maximum uncertainty of the activity rate. Fig. 3 shows that for large values of the product $\eta\gamma$, the MMSE essentially depends on the minimum distance between the inactivity symbol $\{0\}$ and the data symbols $\{-1, 1\}$, and

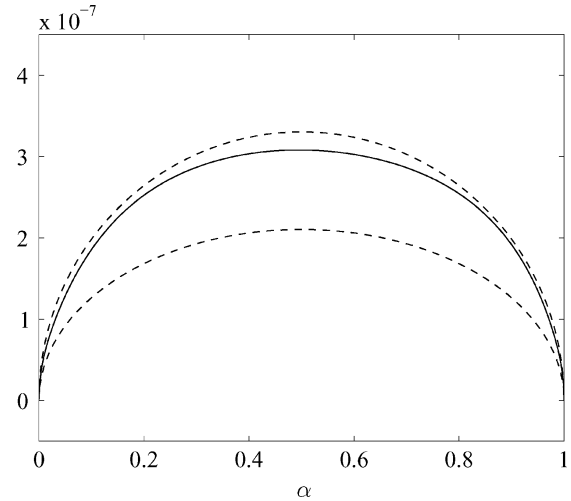


Fig. 3. A comparison of the exact MMSE value with its upper and lower bounds for $\eta\gamma = 20$ dB and $\alpha \in [0, 1]$.

thus users' identification prevails over data detection. Summarizing, the dependence of the MMSE must be symmetrical with respect to $\alpha = 1/2$, since it reflects the impact of prior knowledge about the user's activity into the estimation.

IV. MAXIMUM SYSTEM LOAD AND RELATED CONSIDERATIONS

Recall the definition of maximum system load $\beta = \frac{K}{N}$, where K is the maximum number of users accessing the multiuser channel. When the number of active users is unknown, and there is *a priori* knowledge of the activity rate, the actual system load is $\beta' = \alpha\beta$. In this section, we focus on β and study some of its properties. Notice that, given an activity rate, results for the actual system load follow trivially.

A. Solutions to the Large-System Fixed-Point Equation

We characterize the behavior of the maximum system load subject to quality-of-service constraints. This helps to shed light into the nature of the solutions of the fixed-point equation (13). In particular, there might be cases where (13) has multiple solutions. These solutions correspond to the solutions appearing in any simple mathematical model of magnetism based on the evaluation of the free energy with the fixed-point method [11]. They represent what in the statistical physics parlance is called *phase coexistence* (for example, this occurs in ice or liquid phase of water at 0°C). In particular, at low temperatures, the magnetic system might have three different solutions $0 \leq \Psi_1 < \Psi_2 < \Psi_3 \leq 1$. Solutions Ψ_1 and Ψ_3 are stable: one of them is globally stable (it actually minimizes the free energy), whereas the other is metastable, and a local minimum. Solution Ψ_2 is always unstable, since it is a local maximum. The "true" solution is therefore given by Ψ_1 and Ψ_3 , for which the free energy is globally minimized. The same consideration applies also to our multiuser detection problem where multiuser efficiencies for the IO detector might vary significantly depending on the value of the system load and SNR. More specifically, for sufficiently large SNR, stable solutions may switch between a region that approaches the single-user performance ($\eta = 1 - \epsilon_1$) and a region approaching the worst performance ($\eta = \epsilon_0$), for

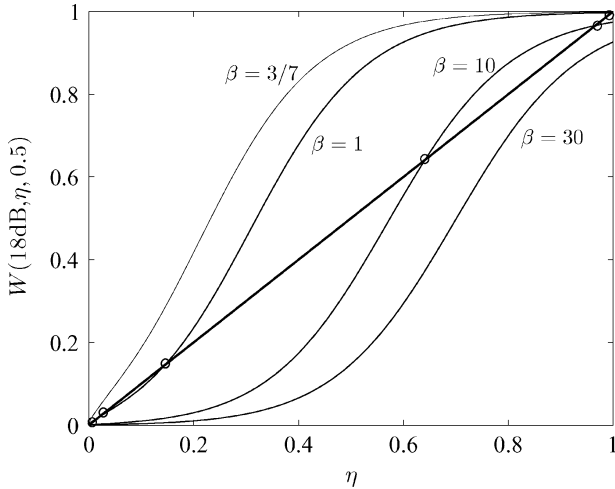


Fig. 4. Fixed-point solutions (marked by circles) for different values of β and fixed $\alpha = 0.5$, and $\gamma = 18$ dB.

$0 < \epsilon_1, \epsilon_0 \ll 1$. Following previous literature [8], we shall call the former solutions *good* and the latter *bad*. When the solution is unique, due to low or high system load, the multiuser efficiency is a globally stable solution that lies in either the good or the bad solution region. Then, for given system parameters, the set of *operational* (or globally stable) solutions is formed by solutions that are part of these sets and minimize the free energy.

The existence of good and bad solutions are critical in our problem. From a computational perspective, we are particularly interested in single solutions, either bad or good, that surely avoid metastability and instability. These solutions belong to a specific subregion within the bad and good regions, and appear for low and high SNR, respectively.

From an information-theoretic perspective, it might seem that the true solutions should capture all our attention. However, it has been shown that metastable solutions appear in suboptimal belief-propagation-based multiuser detectors, where the system is easily attracted into the bad solutions region (corresponding to low multiuser efficiency), due to initial configurations that are far from the true solution [12]. Moreover, the region of good solutions is of interest in the high-SNR analysis, because, for a given system load, it can be observed that the multiuser efficiency tends to 1, consistently with previous theoretical results [23].

Of special interest is the case of single good solutions for which the results arising from the replica method can be rigorously validated [26], [27]. In what follows, we provide an analysis of the boundaries of the stable solution regions, as well as their single-solution subregions with practical interest in the low and high SNR regimes.

A quantitative illustration of the above considerations is provided by plotting the left- and right-hand side (RHS) of (13) to obtain fixed points for constant values of amplitude and activity rate, and as a function of the system load. The solutions of (13) are found at the intersection of the curve corresponding to the RHS with the $y = \eta$ line. Fig. 4 plots different solutions of the RHS of (13) for increasing system load, $\alpha = 0.5$ and $\gamma = 18$ dB

$$W(\gamma, \eta, \alpha) \triangleq \frac{1}{1 + \beta\gamma \text{MMSE}(\eta\gamma, \alpha)}.$$

Notice first that the structure of the fixed-point equation in general does not allow the solution $\eta = 0$, and for finite γ and β , $\eta = 1$ is not a solution. In fact, the latter is an asymptotic solution for large SNR and certain system loads, as the MMSE decays exponentially to 0. From Fig. 4, one can observe the presence of phase transitions and the coexistence of multiple solutions. In particular, we observe that for $\beta = 3/7$ the good solution is computationally feasible. On the other hand, for $\beta = 1$ and $\beta = 10$ the system has three solutions, where the true solution belongs to either the bad or the good solution region. When the system load achieves $\beta = 30$, the curve only intersects the identity curve near 0, and the operational solution is unique and lies in a subregion of bad solutions.

B. System Load and the Space of Fixed-Point Solutions

Even in the case of good solutions, the multiuser efficiency can be greatly degraded by the joint effect of the activity rate and the maximum system load. In order to analyze the fixed-point equation (13) from a different perspective and shed light into the interplay between these parameters, we express the maximum system load as the following function, derived from (13)

$$\Upsilon_\beta(\gamma, \eta, \alpha) \triangleq \frac{(1 - \eta)}{\eta\gamma \text{MMSE}(\eta\gamma, \alpha)}. \quad (17)$$

Since MMSE is a continuous function of η [10], then Υ_β is also a continuous function in any compact set over the domain $\eta \in (0, 1]$ for given SNR and activity rate. It is also easy to observe that, for small values of η , Υ_β tends to infinity regardless of γ and α , whereas in the high- η region, which is of interest here, it decays to 0. Before analyzing the behavior of (17), we introduce a few definitions that help describe the boundaries between the regions with and without coexistence (in the statistical-physics literature, these boundaries are called *spinodal lines* [8]). We also define appropriately the regions of potentially stable solutions as introduced before.

Definition 4.1: The *critical system load* $\beta^*(\gamma, \alpha)$ is the maximum load at which a stable good solution of (13) exists.

Definition 4.2: The *transition system load* $\beta_*(\gamma, \alpha)$ is the minimum load at which the true solution of (13), η_* coexists with other solutions η'_* .

Definition 4.3: The *good solution region* corresponds to the domain of (17) formed by the maximum η in every set of pre-images of Υ_β below the critical system load

$$\mathcal{R}_g = \left\{ \eta \in [0, 1], \eta = \max \left\{ \Upsilon_\beta^{-1}(\beta) \right\}, \forall \beta \in [0, \beta^*] \right\} \quad (18)$$

Similarly, the *bad solution region* corresponds to the domain of (17) formed by the minimum η in every set of pre-images of Υ_β above the transition system load

$$\mathcal{R}_b = \left\{ \eta \in [0, 1], \eta = \min \left\{ \Upsilon_\beta^{-1}(\beta) \right\}, \forall \beta \in [\beta_*, +\infty) \right\}. \quad (19)$$

Definition 4.4: The *single good solution region* $\mathcal{R}_{gc} \subset \mathcal{R}_g$ corresponds to the domain of (17) formed by the pre-image of Υ_β below the transition system load:

$$\mathcal{R}_{gc} = \left\{ \eta \in [0, 1], \eta = \Upsilon_\beta^{-1}(\beta_*), \forall \beta \in [0, \beta_*] \right\} \quad (20)$$

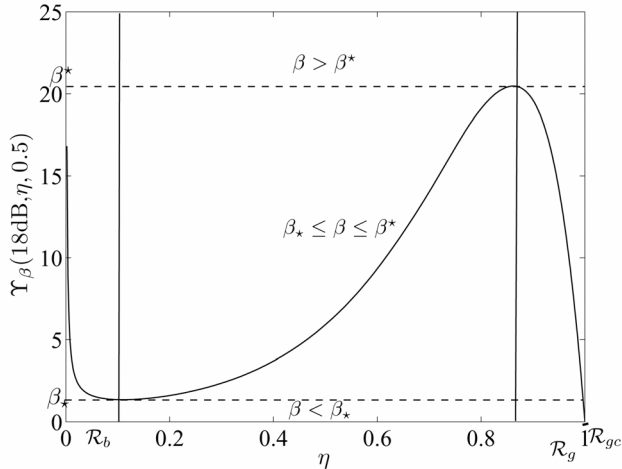


Fig. 5. System load function in the multiuser efficiency domain for $\alpha = 0.5$ and $\gamma = 18$ dB.

and the *single bad solution region* $\mathcal{R}_{bc} \subset \mathcal{R}_b$ corresponds to the domain of (17) formed by the pre-image of Υ_β above the critical system load

$$\mathcal{R}_{bc} = \left\{ \eta \in [0, 1], \eta = \Upsilon_\beta^{-1}(\beta), \forall \beta \in [\beta^*, +\infty) \right\}. \quad (21)$$

Fig. 5 illustrates Υ_β (for fixed SNR and activity rate) and show the regions defined by the aforementioned parameters. It is important to remark that both system loads defined above delimit the regions from which there is phase coexistence ($\beta_* \leq \beta \leq \beta^*$) from the areas where there is one solution ($\beta > \beta^*$ or $\beta < \beta_*$). Additionally, Fig. 5 illustrates the set of solutions that satisfy (20).

Fig. 5 illustrates that it seems useful to define analytically the domain where stable solutions can be found. Beforehand, we differentiate for convenience the case with unknown number of users $\alpha \in (0, 1)$, from the case where all users are active ($\alpha = 1$). We do not consider the case $\alpha = 0$.

1) *Case $\alpha \in (0, 1)$:* In order to analyze the conditions on the system load, SNR, and activity rate, for which we can find a good solution, we use the asymptotic results on the MMSE (16), yielding lower and upper bounds $L(\cdot) \leq \Upsilon_\beta(\gamma, \eta, \alpha) \leq U(\cdot)$ for large enough $\eta\gamma$, where

$$L(\gamma, \eta, \alpha) \triangleq \frac{(1-\eta)}{\sqrt{\pi\eta\gamma\alpha(1-\alpha)}} e^{\eta\gamma/8} \quad (22)$$

$$U(\gamma, \eta, \alpha) \triangleq \frac{(1-\eta)}{2} \sqrt{\frac{\pi}{\eta\gamma\alpha(1-\alpha)}} e^{\eta\gamma/8}. \quad (23)$$

Although not exact for low SNR, the dependence on η of the upper and lower bound provides a good approximation for the dependence of Υ_β for large SNR and given α . Hence, by using $U(\cdot)$ and $L(\cdot)$, we obtain necessary and sufficient conditions that determine the regions of stable solutions and provide analytical expressions for the transition and critical system loads. The main result for $\alpha \in (0, 1)$ follows.

Theorem 4.5: Given the range of activity rates $\alpha \in (0, 1)$, a necessary condition for phase coexistence is

$$\gamma \geq 4(3 + 2\sqrt{2}), \quad (\gamma \geq 13.67 \text{ dB}). \quad (24)$$

Moreover, for high SNR, the condition is met and the transition system load is bounded by

$$L(\gamma, \eta_m, \alpha) < \beta_*(\gamma, \alpha) < U(\gamma, \eta_m, \alpha) \quad (25)$$

while the critical system load is bounded by

$$L(\gamma, \eta_M, \alpha) < \beta^*(\gamma, \alpha) < U(\gamma, \eta_M, \alpha) \quad (26)$$

and η_m, η_M are given by

$$\eta_m \triangleq (\gamma/2 - 2 - 4\Delta(\gamma))/\gamma$$

$$\eta_M \triangleq (\gamma/2 - 2 + 4\Delta(\gamma))/\gamma$$

where $\Delta(\gamma) = \sqrt{(\gamma/8)^2 - 3\gamma/8 + 1/4}$.

Hence, the bad-solution region is given by $\mathcal{R}_b = (0, \eta_m]$, whereas the good-solution region is $\mathcal{R}_g = [\eta_M, 1]$. Similarly, the subregion of single bad solutions $\mathcal{R}_{bc} = (0, \eta_{bc}) \subset \mathcal{R}_b$, and that of single good solutions, $\mathcal{R}_{gc} = (\eta_{gc}, 1] \subset \mathcal{R}_g$, satisfy

$$\eta_{bc} = \min \left\{ \Upsilon_\beta^{-1}(\beta^*) \right\} > \eta_{bc}^*$$

$$\eta_{gc} = \max \left\{ \Upsilon_\beta^{-1}(\beta_*) \right\} < \eta_{gc}^*$$

where $\eta_{bc}^* \triangleq \min\{U^{-1}(\beta^*)\}$, and $\eta_{gc}^* \triangleq \max\{L^{-1}(\beta_*)\}$ are obtained from the bounds.

Proof: See Appendix III. ■

The above result provides the general boundaries of the space of solutions of our problem. It is important to note that η_m and η_M are very good approximations for high SNR of the positions of the local minimum and maximum observed in Fig. 5, which determine the transition and the critical system loads. As a consequence, remark that Theorem 4.5 analytically tells us the range of β 's for which there are either single or multiple solutions based on the up-to-a-constant approximation of Υ_β by (22) and (23). Similarly, η_{bc}^* and η_{gc}^* are tight bounds of the boundaries of the single-solution regions as $U(\cdot)$ and $L(\cdot)$ are of $\Upsilon_\beta(\cdot)$. Note also that the activity rate affects the system load boundaries in the same symmetrical manner as it does the MMSE (i.e., the worst case here also corresponds to $\alpha = 0.5$) but has no impact on the regions of good and bad solutions, that are only reduced in size by increasing the SNR. In particular, these regions are characterized, in the limit of high SNR, as follows.

Corollary 4.6: In the limit of high SNR, $\mathcal{R}_g \rightarrow \{1\}$, $\mathcal{R}_b \rightarrow \{0\}$, and consequently $\mathcal{R}_{gc} \rightarrow \{1\}$, and $\mathcal{R}_{bc} \rightarrow \{0\}$.

Proof: The above corollary results from

$$\lim_{\gamma \rightarrow \infty} \eta_M = \lim_{\gamma \rightarrow \infty} \frac{(\gamma/2 - 2 + 4\sqrt{(\gamma/8)^2 - 3\gamma/8 + 1/4})}{\gamma}$$

$$= 1$$

$$\lim_{\gamma \rightarrow \infty} \eta_m = \lim_{\gamma \rightarrow \infty} \frac{(\gamma/2 - 2 - 4\sqrt{(\gamma/8)^2 - 3\gamma/8 + 1/4})}{\gamma}$$

$$= 0. \quad \blacksquare$$

Note that, given a system load β with $\beta^* > \beta$, for sufficiently large SNR the unique true (large-system) solution is $\eta = 1$, which corroborates the main result in [23]. Moreover, the description of the single good solutions by analytical means allows

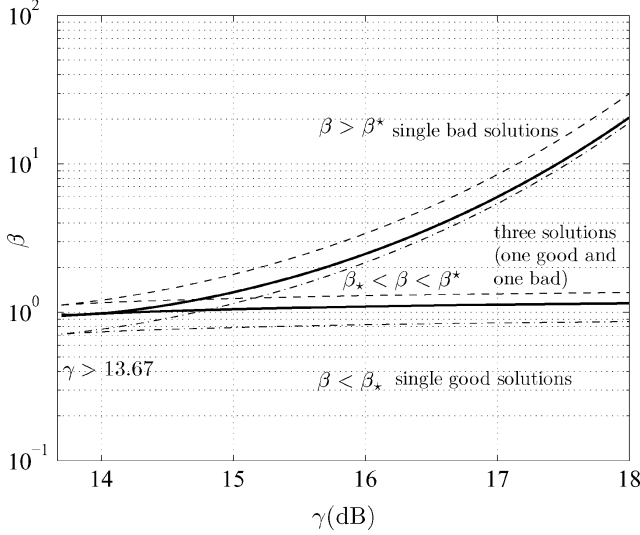


Fig. 6. Upper and lower bounds on the numerical spinodal lines (thick line) for $\alpha = 0.5$.

the computation of a sufficient condition on the system load to guarantee a given multiuser efficiency in practical implementations. More specifically, we use the aforementioned lower bound on Υ to state that any system load below $L(\cdot)$ guarantees that the given multiuser efficiency is achieved. The result is stated as follows.

Corollary 4.7: The maximum system load $\beta_{\alpha,\eta}$ for a given activity rate and multiuser efficiency requirement $\eta = 1 - \epsilon$, where $0 < \epsilon \ll 1$, that lies in R_{ge} , is lower-bounded in the high-SNR region by

$$\beta_{\alpha,\eta} > \frac{\epsilon}{\sqrt{\pi\eta\gamma\alpha(1-\alpha)}} e^{(1-\epsilon)\gamma/8}. \quad (27)$$

In Fig. 6 we show the numerical values of the transition and the critical system load as a function of the SNR in the (γ, β) space. We also use the asymptotic expansion to derive upper and lower bounds, respectively. The plotted curves are the *spinodal lines*, which mark the boundary between the regions with and without solution coexistence. The β_* (lower branch) separates the region where the bad solution disappears, whereas β^* (upper branch) contains the bifurcation points at which any good solution disappears. The intersection point between both branches corresponds to the SNR threshold (24), which provides the necessary condition for solution coexistence.

2) *Case $\alpha = 1$:* We now apply the same reasoning for the “classical” approach to multiuser detection, corresponding to activity rate 1. In this case, using the approximation in [30], the system load function can be lower-bounded by

$$\Upsilon_{\beta}(\gamma, \eta, 1) = \frac{(1-\eta)}{\eta\gamma\text{MMSE}(\eta\gamma, 1)} < \frac{(1-\eta)e^{\eta\gamma/2}}{\sqrt{\pi\eta\gamma}}. \quad (28)$$

Hence, we can derive the following spinodal lines.

Corollary 4.8: Given $\alpha = 1$ a necessary condition for the phase coexistence is that

$$\gamma \geq 3 + 2\sqrt{2}, \quad (\gamma \geq 7.65 \text{ dB}).$$

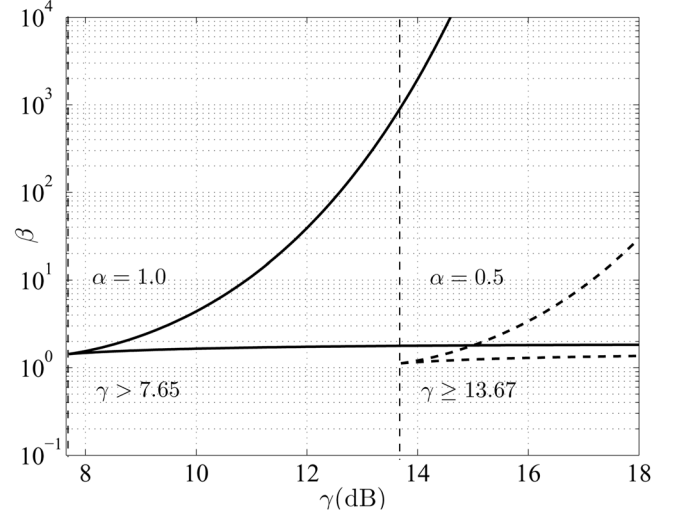


Fig. 7. Comparison of upper bounds on the spinodal lines for $\alpha = 1.0$ (left) and $\alpha = 0.5$ (right).

Moreover, for high SNR, the condition is met and the transition system load is upper-bounded by

$$\beta_* < \frac{(1-\eta_{m'})}{2} \sqrt{\frac{\pi}{\eta_{m'}\gamma}} e^{\frac{\eta_{m'}\gamma}{2}} \quad (29)$$

and the critical system load is upper-bounded by

$$\beta^* < \frac{(1-\eta_{M'})}{2} \sqrt{\frac{\pi}{\eta_{M'}\gamma}} e^{\frac{\eta_{M'}\gamma}{2}}, \quad (30)$$

where $\eta_{m'}$ and $\eta_{M'}$ are given by

$$\eta_{m'} \triangleq \frac{(\gamma/2 - 1/2 - \Lambda(\gamma))}{\gamma}$$

$$\eta_{M'} \triangleq \frac{(\gamma/2 - 1/2 + \Lambda(\gamma))}{\gamma}$$

and $\Lambda(\gamma) = \sqrt{(\gamma/2)^2 - 3\gamma/2 + 1/4}$.

Hence, the bad solution region is given by $\mathcal{R}_b = (0, \eta_{m'})$ whereas the good solution region is $\mathcal{R}_g = [\eta_{M'}, 1]$.

Proof: The proof is analogous to that of Theorem 4.5. ■

The same consequence for the asymptotic operational region holds here.

Corollary 4.9: In the limit of high SNR, $\mathcal{R}_g \rightarrow \{1\}$, and $\mathcal{R}_b \rightarrow \{0\}$.

Proof: This corollary results from

$$\lim_{\gamma \rightarrow \infty} \eta_{M'} = \lim_{\gamma \rightarrow \infty} \frac{(\gamma/2 - 1/2 + \sqrt{(\gamma/2)^2 - 3\gamma/2 + 1/4})}{\gamma} = 1$$

$$\lim_{\gamma \rightarrow \infty} \eta_{m'} = \lim_{\gamma \rightarrow \infty} \frac{(\gamma/2 - 1/2 - \sqrt{(\gamma/2)^2 - 3\gamma/2 + 1/4})}{\gamma} = 0.$$

In Fig. 7, one can observe a 6 dB-difference between the spinodal lines corresponding to $\alpha = 0.5$ and to $\alpha = 1.0$. This is due to the minimum distance of the underlying constellations, which causes the MMSE to have different exponential decays. This can

be interpreted by saying that the addition of activity detection to data detection is reflected by a 6 dB increase of the SNR needed to achieve the same system load performance. Moreover, with $\alpha < 1$, the transition system load is lower than the case where all users are active, and, therefore, computationally good solutions correspond to lower values of the maximum system load.

C. Maximum System Load With Error Probability Constraints

A natural application of the above results to practical designs appears when the quality-of-service requirements of the system are specified in terms of uncoded error probability. Such an application can provide some extra insight into the plausible values of β with joint activity and data detection for efficient design of large CDMA systems. Once a multiuser-efficiency requirement is assigned, the corresponding probability of error follows naturally. Note first that, in order to detect the activity as well as the transmitted data, our model deals with a ternary constellation $\{-1, 0, 1\}$. When any of these symbols is transmitted by each user with constant SNR $= \gamma$ through a bank of large-system equivalent white Gaussian noise channels with variance $1/\eta$, the probability of error over \mathcal{X} depends on the prior probabilities as well as the Euclidean distance between the symbols. The error probability implied by the replica analysis is

$$P_e(\eta, \gamma, \alpha) = 2(1 - \alpha)Q\left(\frac{\sqrt{\eta\gamma}}{2} + \frac{\lambda_\alpha}{\sqrt{\eta\gamma}}\right) + \alpha Q\left(\frac{\sqrt{\eta\gamma}}{2} - \frac{\lambda_\alpha}{\sqrt{\eta\gamma}}\right), \quad (31)$$

where $Q(x) \triangleq \frac{1}{\sqrt{2\pi}} \int_x^\infty e^{-\frac{t^2}{2}} dt$ is the Gaussian tail function, and $\lambda_\alpha \triangleq \ln\left(\frac{2(1-\alpha)}{\alpha}\right)$.

The relationship between η and P_e for our particular case can be used to reformulate the bounds on the function Υ_β in terms of error probability.

Corollary 4.10: The maximum system load $\Upsilon_\beta(\eta, \gamma, \alpha)$ for a given error probability P_e , γ , and activity rate is bounded for high SNR by

$$L(\gamma, \eta_{\max}, \alpha) < \Upsilon_\beta(\eta_{\max}, \gamma, \alpha) < U(\gamma, \eta_{\max}, \alpha), \quad (32)$$

where

$$\eta_{\max} \triangleq \max\{\eta_P, \eta_{gc}\},$$

and (η_P, γ, α) is the pre-image of P_e .

Proof: The result is obtained by noticing that the multiuser efficiency requirement extracted from P_e must lie on the subregion $(\eta_{gc}, 1]$. ■

Notice that, if the error probability satisfies $\eta_p \leq \eta_{gc} = \eta_{\max}$, then the constraint is described by the bounds on the transition load (26). However, if $\eta_{gc} < \eta_p = \eta_{\max}$, then, for Corollary 4.7, the maximum system load can be also easily bounded. Fig. 8 plots the critical system load for two different error probabilities requirements and three different activity rates.

V. CONCLUSION

We have analyzed multiuser detectors for CDMA where the fraction of active users is unknown, and must be estimated in

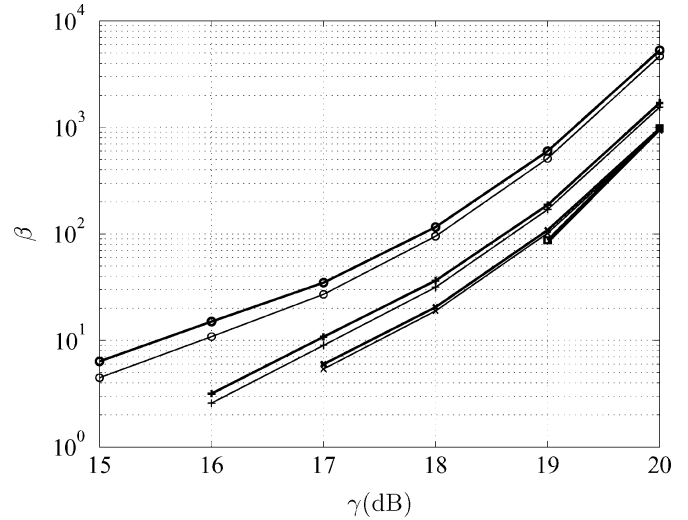


Fig. 8. Critical system load for different uncoded error probabilities and activity rates. Thicker lines represent numerical results, whereas regular lines show the corresponding lower bounds. Lines with circle markers: $P_e = 10^{-3}$ and $\alpha = 0.99$. Lines with cross markers: $P_e = 10^{-3}$ and $\alpha = 0.1$. Lines with star markers: $P_e = 10^{-3}$ and $\alpha = 0.5$. Lines with square markers: error probability 10^{-5} and $\alpha = 0.5$.

a tracking phase. Using a large-system approach and statistical-physics tools, we have derived a fixed-point equation for the optimal user-and-data detector, and provided asymptotic bounds for the corresponding MMSE. Further, we have described the space of stable solutions of the fixed-point equation, and derived explicit bounds on the critical and transition system loads for all users' activity rates. These are consistent with the results obtained under the classic multiuser-detection assumption ($\alpha = 1.0$) made in the literature. The study of the so-called spinodal lines allowed us to determine the regions of stable good and bad solutions, including subregions of single solutions (also computationally feasible), in the system load versus SNR parameter space of our model. Our results show that for a user-and-data detector, the boundaries of the space of solutions do depend on the activity rate, whereas the regions of stable solutions (good and bad) are only affected by the SNR. Hence, the overall system load performance keeps a symmetric behavior with respect to α . In practical implementations with high quality-of-service demands, we are interested in maximizing the critical system load, while keeping the optimal detector in the feasible subregion of good multiuser efficiencies, such that a wider range of potential users can successfully access the channel with a given rate. By increasing the SNR, this goal can be achieved, but for limited SNR, the certainty on the users' activity allows allocation of more users for a given spreading length. A relevant example corresponds to a system with a given error probability requirement. For this case, we have shown that, for sufficiently large SNR, we can choose the multiuser efficiency in the domain of feasible good solutions, and maximize the critical system accordingly.

One of the assumptions of this paper is to model the activity as an i.i.d. process. Further extensions of this work to non-i.i.d. scenarios can be found in [5] where the users' activity evolves according to a Markov process and in [31], where users transmit encoded messages and the activity is correlated over the coded blocks of each user.

APPENDIX I
PROOF OF COROLLARY 3.1

We first derive the MMSE for our particular ternary input distribution in the general fixed-point equation (9) (see the equation at the bottom of the page).

After appropriate change of variables the MMSE is

$$\text{MMSE}(\eta\gamma, \alpha) = \alpha - \int \frac{1}{\sqrt{2\pi}} e^{-\frac{y^2}{2}} \times \frac{\alpha^2 \sinh[\eta\gamma - y\sqrt{\eta\gamma}]}{\alpha \cosh[\eta\gamma - y\sqrt{\eta\gamma}] + (1-\alpha)e^{\eta\gamma/2}} dy.$$

Since the SNR is constant among users, it follows naturally that the large-system fixed-point equation is given by (13).

APPENDIX II
PROOF OF THEOREM 3.3

From now on, we omit the explicit indication of the arguments of the MMSE function. The lower bound is obtained by noting that, for large SNR, the general MMSE, denoted MMSE_α , is lower-bounded by $\text{MMSE}_{\{0,1\}}$, which describes the detection performance when the transmitted symbols are $\{0, 1\}$, with probabilities $\{1 - \alpha, \alpha\}$. In this case the MMSE has the following form

$$\text{MMSE}_{\{0,1\}} = \alpha - \int \frac{\left(\sqrt{\frac{\eta}{2\pi}} \alpha e^{-\frac{\eta}{2}(y-\sqrt{\gamma})^2}\right)^2}{\sqrt{\frac{\eta}{2\pi}} (\alpha e^{-\frac{\eta}{2}(y-\sqrt{\gamma})^2} + (1-\alpha)e^{-\frac{\eta}{2}y^2})} dy$$

where $\lambda_\alpha \triangleq \frac{1}{2} \ln\left(\frac{1-\alpha}{\alpha}\right)$. After some manipulation and appropriate changes of variables, we obtain

$$\text{MMSE}_{\{0,1\}} = \alpha - \alpha e^{-\frac{3\eta\gamma}{8} - \lambda_\alpha} \times \sqrt{\frac{1}{2\pi}} \int_{-\infty}^{\infty} e^{-\frac{1}{2}(2z - \sqrt{\eta\gamma} + \frac{2\lambda_\alpha}{\sqrt{\eta\gamma}})^2} \text{sech}(z\sqrt{\eta\gamma}) dz.$$

Use now the following asymptotic expansion for $\text{sech}(z): |z| \rightarrow \infty$

$$\text{sech}(z) = 2e^{-|z|} \left(1 + \sum_{\ell=1}^{\infty} (-1)^\ell e^{-2\ell|z|}\right)$$

and obtain

$$\begin{aligned} \text{MMSE}_{\{0,1\}} &= \alpha - \alpha e^{-\frac{3\eta\gamma}{8} - \lambda_\alpha} \sqrt{\frac{1}{2\pi}} \left[\int_{-\infty}^0 e^{-\frac{1}{2}(2z - \sqrt{\eta\gamma} + \frac{2\lambda_\alpha}{\sqrt{\eta\gamma}})^2} \right. \\ &\quad \times 2e^{z\sqrt{\eta\gamma}} \left(1 + \sum_{\ell=1}^{\infty} (-1)^\ell e^{2\ell z\sqrt{\eta\gamma}}\right) dz \\ &\quad + \int_0^{\infty} e^{-\frac{1}{2}(2z - \sqrt{\eta\gamma} + \frac{2\lambda_\alpha}{\sqrt{\eta\gamma}})^2} 2e^{-z\sqrt{\eta\gamma}} \\ &\quad \times \left(1 + \sum_{\ell=1}^{\infty} (-1)^\ell e^{-2\ell z\sqrt{\eta\gamma}}\right) dz \left. \right]. \end{aligned}$$

We now use the expansion

$$\begin{aligned} \text{MMSE}_{\{0,1\}} &= \alpha - \alpha e^{-\eta\gamma/8 + \lambda_\alpha - \frac{2\lambda_\alpha^2}{\eta\gamma}} \\ &\quad \times \left[\sum_{\ell=0}^{\infty} (-1)^\ell \sqrt{\frac{2}{\pi}} \int_{-\infty}^0 e^{-2z^2 + ((3+2\ell)\sqrt{\eta\gamma} - \frac{4\lambda_\alpha}{\sqrt{\eta\gamma}})z} dz \right. \\ &\quad \left. + \sum_{\ell=0}^{\infty} (-1)^\ell \sqrt{\frac{2}{\pi}} \int_0^{\infty} e^{-2z^2 + ((1-2\ell)\sqrt{\eta\gamma} - \frac{4\lambda_\alpha}{\sqrt{\eta\gamma}})z} dz \right]. \end{aligned}$$

Express now the integrals in terms of the Q-function, $Q(x) \triangleq \frac{1}{\sqrt{2\pi}} \int_x^{\infty} e^{-\frac{t^2}{2}} dt$

$$\begin{aligned} \text{MMSE}_{\{0,1\}} &= \alpha e^{-\eta\gamma/8 + \lambda_\alpha - \frac{2\lambda_\alpha^2}{\eta\gamma}} \left[e^{\frac{(\frac{\sqrt{\eta\gamma}}{2} - \frac{2\lambda_\alpha}{\sqrt{\eta\gamma}})^2}{2}} Q\left(\frac{\sqrt{\eta\gamma}}{2} - \frac{2\lambda_\alpha}{\sqrt{\eta\gamma}}\right) \right. \\ &\quad - e^{\frac{(\frac{3\sqrt{\eta\gamma}}{2} - \frac{2\lambda_\alpha}{\sqrt{\eta\gamma}})^2}{2}} Q\left(\frac{3\sqrt{\eta\gamma}}{2} - \frac{2\lambda_\alpha}{\sqrt{\eta\gamma}}\right) - \sum_{\ell=1}^{\infty} (-1)^\ell \\ &\quad \times \left[e^{\frac{(\frac{(2\ell-1)\sqrt{\eta\gamma}}{2} + \frac{2\lambda_\alpha}{\sqrt{\eta\gamma}})^2}{2}} Q\left(\frac{(2\ell-1)\sqrt{\eta\gamma}}{2} + \frac{2\lambda_\alpha}{\sqrt{\eta\gamma}}\right) \right. \\ &\quad \left. + e^{\frac{(\frac{(3+2\ell)\sqrt{\eta\gamma}}{2} - \frac{2\lambda_\alpha}{\sqrt{\eta\gamma}})^2}{2}} \right. \\ &\quad \left. \times \left(Q\left(\frac{(3+2\ell)\sqrt{\eta\gamma}}{2} - \frac{2\lambda_\alpha}{\sqrt{\eta\gamma}}\right) \right) \right] \left. \right]. \end{aligned}$$

$$\begin{aligned} \text{MMSE}(\eta\gamma, \alpha) &= \mathbb{E} \left[(\mathbf{b}^k - \mathbb{E}\{\mathbf{b}^k | \mathcal{S}, y\})^2 \right] \\ &= \alpha - \int \frac{\mathbb{E}_{\mathbf{b}^k}^2 \{ \mathbf{b}^k P(y | \eta, \mathbf{b}^k, \mathcal{S}) \}}{\mathbb{E}_{\mathbf{b}^k} \{ P(y | \eta, \mathbf{b}^k, \mathcal{S}) \}} dy \\ &= \alpha - \int \frac{\left(\sqrt{\frac{\eta}{2\pi}} \frac{\alpha}{2} \left[e^{-\frac{\eta}{2}(y-\sqrt{\gamma})^2} - e^{-\frac{\eta}{2}(y+\sqrt{\gamma})^2} \right] \right)^2}{\sqrt{\frac{\eta}{2\pi}} \left(\frac{\alpha}{2} \left[e^{-\frac{\eta}{2}(y-\sqrt{\gamma})^2} + e^{-\frac{\eta}{2}(y+\sqrt{\gamma})^2} \right] \right) + (1-\alpha)e^{\frac{\eta}{2}y^2}} dy \\ &= \alpha - \frac{1}{2} \sqrt{\frac{\eta}{2\pi}} \left[\int \frac{e^{-\frac{\eta}{2}(y-\sqrt{\gamma})^2} \alpha^2 \sinh(\eta y \sqrt{\gamma})}{\alpha \cosh(\eta y \sqrt{\gamma}) + (1-\alpha)e^{\frac{\eta y^2}{2}}} dy - \int \frac{e^{-\frac{\eta}{2}(y'+\sqrt{\gamma})^2} \alpha^2 \sinh(\eta y' \sqrt{\gamma})}{\alpha \cosh(\eta y' \sqrt{\gamma}) + (1-\alpha)e^{\frac{\eta y'^2}{2}}} dy' \right]. \end{aligned}$$

Next, use the expansion of the Q function, [1]

$$Q(x) = \frac{e^{-x^2/2}}{\sqrt{2\pi x}} \left(1 + \sum_{\ell=1}^{\infty} (-1)^\ell \frac{\prod_{q=1}^{\ell} (2q-1)}{x^{2\ell}} \right) \quad (33)$$

to obtain

$$\begin{aligned} \text{MMSE}_{\{0,1\}} &= 2\sqrt{\frac{\alpha(1-\alpha)}{2\pi\eta\gamma}} e^{-\eta\gamma/8 - \frac{2\lambda_\alpha^2}{\eta\gamma}} \\ &\times \left[\frac{1}{\left(1 - \frac{4\lambda_\alpha}{\eta\gamma}\right)} + \frac{1}{\left(1 + \frac{4\lambda_\alpha}{\eta\gamma}\right)} - \frac{1}{\left(3 - \frac{4\lambda_\alpha}{\eta\gamma}\right)} \right. \\ &\quad \left. - \frac{1}{\left(3 + \frac{4\lambda_\alpha}{\eta\gamma}\right)} + \dots + \mathcal{O}\left(\frac{1}{\sqrt{\eta\gamma}}\right) \right] \end{aligned}$$

where the linear term in λ_α is substituted in the common factor. Assuming a large value $\eta\gamma$, and using the result

$$2 \sum_{n=0}^{\infty} \frac{(-1)^{n+1}}{2n+1} = \frac{\pi}{2}$$

we obtain the following lower bound:

$$\begin{aligned} \text{MMSE}_{\{0,1\}} &> 2\sqrt{\frac{\alpha(1-\alpha)}{2\pi\eta\gamma}} e^{-\eta\gamma/8} \sqrt{2} \\ &= 2\sqrt{\frac{\alpha(1-\alpha)}{\pi\eta\gamma}} e^{-\eta\gamma/8}. \end{aligned}$$

As far as the upper-bound is concerned, we derive the general MMSE, denoted MMSE_{α} , and its particular case when all users are assumed to be active, denoted MMSE_1 . Hence, we express the corresponding integrals in an analogous manner

$$\begin{aligned} \zeta_\alpha &= \int \frac{1}{\sqrt{2\pi}} e^{-\frac{(y-\sqrt{\eta\gamma})^2}{2}} \frac{\alpha \sinh(y\sqrt{\eta\gamma})}{\alpha \cosh(y\sqrt{\eta\gamma}) + (1-\alpha)e^{\eta\gamma/2}} dy. \\ \zeta_1 &= \int \frac{1}{\sqrt{2\pi}} e^{-\frac{(y-\sqrt{\eta\gamma})^2}{2}} \tanh(y\sqrt{\eta\gamma}) dy. \end{aligned}$$

We now obtain

$$\begin{aligned} \text{MMSE}_{\alpha} &= \alpha(1 - \zeta_\alpha) = \alpha(1 + \zeta_1 - \zeta_1 - \zeta_\alpha) \\ &= \alpha((1 - \zeta_1) + (\zeta_1 - \zeta_\alpha)) \\ &= \alpha(\text{MMSE}_1 + (\zeta_1 - \zeta_\alpha)) \end{aligned}$$

Next, we expand $\alpha(\zeta_1 - \zeta_\alpha)$, which yields

$$\begin{aligned} \alpha(\zeta_1 - \zeta_\alpha) &= (1-\alpha)e^{\eta\gamma/2} \int \frac{1}{\sqrt{2\pi}} e^{-\frac{(y-\sqrt{\eta\gamma})^2}{2}} \\ &\times \frac{\alpha \sinh[y\sqrt{\eta\gamma}]}{\alpha \cosh^2[y\sqrt{\eta\gamma}] + (1-\alpha)e^{\eta\gamma/2} \cosh(y\sqrt{\eta\gamma})} dy \\ &= (1-\alpha)e^{\eta\gamma/2} \int \frac{1}{\sqrt{2\pi}} e^{-\frac{(y-\sqrt{\eta\gamma})^2}{2}} \\ &\times \frac{\tanh[y\sqrt{\eta\gamma}]}{\cosh[y\sqrt{\eta\gamma}] + e^{\eta\gamma/2 + \ln(\frac{1-\alpha}{\alpha})}} dy \quad (34) \end{aligned}$$

Consider now the following inequalities:

$$\tanh(z) \leq 1 \quad \text{and} \quad \cosh(z) \geq \frac{e^z}{2}.$$

After substitution and manipulation of the denominator of (34), we obtain

$$\begin{aligned} \alpha(\zeta_1 - \zeta_\alpha) &\leq (1-\alpha)e^{\eta\gamma/2} \\ &\times \int_{-\infty}^{\infty} \frac{e^{-\frac{(y-\sqrt{\eta\gamma})^2}{2}}}{\sqrt{2\pi}} \frac{1}{\frac{e^{y\sqrt{\eta\gamma}}}{2} + e^{\eta\gamma/2 + \ln(\frac{1-\alpha}{\alpha})}} dy \\ &= (1-\alpha)e^{\eta\gamma/2} \\ &\times \int_{-\infty}^{\infty} \frac{e^{-\frac{(y-\sqrt{\eta\gamma})^2}{2}}}{\sqrt{2\pi}} \frac{e^{-\frac{y\sqrt{\eta\gamma}}{2} - \frac{\eta\gamma}{4} - \phi_\alpha}}{\cosh\left(\frac{y\sqrt{\eta\gamma}}{2} - \frac{\eta\gamma}{4} - \phi_\alpha\right)} dy \end{aligned}$$

where $\phi_\alpha \triangleq \frac{1}{2} \ln\left(\frac{2(1-\alpha)}{\alpha}\right)$. We readjust terms to express the integral in a convenient form

$$\begin{aligned} \alpha(\zeta_1 - \zeta_\alpha) &\leq (1-\alpha)e^{-\eta\gamma/8 - \phi_\alpha} \int_{-\infty}^{\infty} \frac{e^{-\frac{(y-\sqrt{\eta\gamma})^2}{2}}}{\sqrt{2\pi}} \\ &\times \text{sech}\left(\frac{y\sqrt{\eta\gamma}}{2} - \frac{\eta\gamma}{4} - \phi_\alpha\right) dy. \end{aligned}$$

We now use the following transformation in the variable of integration: $y = 2z + \frac{\sqrt{\eta\gamma}}{2} + \frac{2\phi_\alpha}{\sqrt{\eta\gamma}}$

$$\begin{aligned} \alpha(\zeta_1 - \zeta_\alpha) &\leq 2(1-\alpha)e^{\frac{7\eta\gamma}{8} - \phi_\alpha} \int_{-\infty}^{\infty} \frac{e^{-\frac{(2z - 2\sqrt{\eta\gamma} - \frac{2\phi_\alpha}{\sqrt{\eta\gamma}})^2}{2}}}{\sqrt{2\pi}} \\ &\times \text{sech}(z\sqrt{\eta\gamma}) dz \\ &+ 2(1-\alpha)e^{-\eta\gamma/8 - \phi_\alpha} \\ &\times \int_0^{\infty} \frac{e^{-\frac{(2z + \frac{2\phi_\alpha}{\sqrt{\eta\gamma}})^2}{2}}}{\sqrt{2\pi}} \text{sech}(z\sqrt{\eta\gamma}) dz \end{aligned}$$

and the asymptotic expansion for $\text{sech}(z)$ in the above derivation

$$\text{sech}(z) = 2e^{-|z|} \left(1 + \sum_{\ell=1}^{\infty} (-1)^\ell e^{-2\ell|z|} \right).$$

This yields

$$\begin{aligned} \alpha(\zeta_1 - \zeta_\alpha) &\leq 4(1-\alpha)e^{-\eta\gamma/8 - \phi_\alpha - \frac{2\phi_\alpha^2}{\eta\gamma}} \\ &\times \sum_{\ell=0}^{\infty} (-1)^\ell \int_0^{\infty} \frac{e^{-2z^2 + ((1+2\ell)\sqrt{\eta\gamma} - \frac{4\phi_\alpha}{\sqrt{\eta\gamma}})z}}{\sqrt{2\pi}} dz \\ &+ 4(1-\alpha)e^{-\eta\gamma/8 - \phi_\alpha - \frac{2\phi_\alpha^2}{\eta\gamma}} \\ &\times \sum_{\ell=0}^{\infty} (-1)^\ell \int_0^{\infty} \frac{e^{-2z^2 - ((1+2\ell)\sqrt{\eta\gamma} + \frac{4\phi_\alpha}{\sqrt{\eta\gamma}})z}}{\sqrt{2\pi}} dz. \end{aligned}$$

Finally, expressing the integrals in terms of the Q function

$$\begin{aligned} & \alpha(\zeta_1 - \zeta_\alpha) \\ & \leq 2(1 - \alpha)e^{-\eta\gamma/8 - \phi_\alpha - \frac{2\phi_\alpha^2}{\eta\gamma}} \left[\sum_{\ell=0}^{\infty} (-1)^\ell \right. \\ & \quad \times e^{\frac{((1+2\ell)\sqrt{\eta\gamma} - \frac{2\phi_\alpha}{\sqrt{\eta\gamma}})^2}{2}} Q\left(\frac{(1+2\ell)\sqrt{\eta\gamma}}{2} - \frac{2\phi_\alpha}{\sqrt{\eta\gamma}}\right) \\ & \quad + \sum_{\ell=0}^{\infty} (-1)^\ell e^{\frac{((1+2\ell)\sqrt{\eta\gamma} + \frac{2\phi_\alpha}{\sqrt{\eta\gamma}})^2}{2}} \\ & \quad \left. \times Q\left(\frac{(1+2\ell)\sqrt{\eta\gamma}}{2} + \frac{2\phi_\alpha}{\sqrt{\eta\gamma}}\right) \right] \end{aligned}$$

and manipulating the expansion

$$\begin{aligned} \alpha(\zeta_1 - \zeta_\alpha) & \leq 2(1 - \alpha)e^{-\eta\gamma/8 - \phi_\alpha - \frac{2\phi_\alpha^2}{\eta\gamma}} \\ & \quad \times \left[e^{\frac{(\frac{\sqrt{\eta\gamma}}{2} - \frac{2\phi_\alpha}{\sqrt{\eta\gamma}})^2}{2}} Q\left(\frac{\sqrt{\eta\gamma}}{2} - \frac{2\phi_\alpha}{\sqrt{\eta\gamma}}\right) \right. \\ & \quad + e^{\frac{(\frac{\sqrt{\eta\gamma}}{2} + \frac{2\phi_\alpha}{\sqrt{\eta\gamma}})^2}{2}} Q\left(\frac{\sqrt{\eta\gamma}}{2} + \frac{2\phi_\alpha}{\sqrt{\eta\gamma}}\right) \\ & \quad + \sum_{\ell=1}^{\infty} (-1)^\ell e^{\frac{((1+2\ell)\sqrt{\eta\gamma} - \frac{2\phi_\alpha}{\sqrt{\eta\gamma}})^2}{2}} \\ & \quad \times Q\left(\frac{(1+2\ell)\sqrt{\eta\gamma}}{2} - \frac{2\phi_\alpha}{\sqrt{\eta\gamma}}\right) \\ & \quad + \sum_{\ell=1}^{\infty} (-1)^\ell e^{\frac{((1+2\ell)\sqrt{\eta\gamma} + \frac{2\phi_\alpha}{\sqrt{\eta\gamma}})^2}{2}} \\ & \quad \left. \times Q\left(\frac{(1+2\ell)\sqrt{\eta\gamma}}{2} + \frac{2\phi_\alpha}{\sqrt{\eta\gamma}}\right) \right] \end{aligned}$$

we obtain, after using the series expansion (33)

$$\begin{aligned} & \alpha(\zeta_1 - \zeta_\alpha) \\ & \leq 2\sqrt{\frac{(1-\alpha)\alpha}{\pi\eta\gamma}} e^{-\eta\gamma/8} \left[\frac{1}{\left(1 - \frac{4\phi_\alpha}{\eta\gamma}\right)} + \frac{1}{\left(1 + \frac{4\phi_\alpha}{\eta\gamma}\right)} \right. \\ & \quad \left. - \frac{1}{\left(3 - \frac{4\phi_\alpha}{\eta\gamma}\right)} - \frac{1}{\left(3 + \frac{4\phi_\alpha}{\eta\gamma}\right)} + \dots + \mathcal{O}\left(\frac{1}{\sqrt{\eta\gamma}}\right) \right] \end{aligned}$$

where the linear term in $\phi_\alpha = \frac{1}{2} \ln\left(\frac{2(1-\alpha)}{\alpha}\right)$ is substituted in the common factor, and quadratic terms are neglected.

Using the same result as before on the series $2 \sum_{n=0}^{\infty} \frac{(-1)^{n+1}}{2n+1}$, we obtain the upper bound:

$$\alpha(\zeta_1 - \zeta_\alpha) < \sqrt{\frac{\pi\alpha(1-\alpha)}{\eta\gamma}} e^{-\eta\gamma/8}.$$

Finally, using the upper bound given in Lemma 3.2 for BPSK, the overall MMSE can be upper-bounded by

$$\text{MMSE}_\alpha \leq 2\alpha e^{-\eta\gamma/2} + \sqrt{\frac{\pi\alpha(1-\alpha)}{\eta\gamma}} e^{-\eta\gamma/8}.$$

APPENDIX III

PROOF OF THEOREM 4.5

We analyze the function

$$G(\eta) = (1 - \eta)e^{u\eta}/\sqrt{\eta} \quad (35)$$

where u is a constant, which entirely describes the dependence of Υ_β on η for sufficiently large $\eta\gamma$. By simple derivation of (35), it is easy to observe that the solution has critical points in the domain $(0, 1]$ if and only if $u \geq (3 + \sqrt{8})/2$. These points are

$$\begin{aligned} \eta_m & = \frac{u - 1/2 - \sqrt{u^2 - 3u + 1/4}}{2u} \\ \eta_M & = \frac{u - 1/2 + \sqrt{u^2 - 3u + 1/4}}{2u} \end{aligned}$$

and lie in the domain $(0, 1]$. In fact, note that $u^2 - 3u + 1/4 < (u - 3/2)^2$, and thus it can be verified that $0 < 1/2u < \eta_m < \eta_M < 1 - 1/u < 1$. By using the second derivative of (35) we observe that these solutions correspond to a local minimum and a local maximum, respectively. Let us now study (35) to justify the range of values of the critical system load. $G(\eta)$ is a continuous function in $(0, 1]$ that takes positive values. Since $G(\eta)$ tends to 0 as η approaches 1, and tends to infinity as η approaches 0, it can be concluded that the range for which $G(\eta)$ has only one pre-image is $(0, G(\eta_m)) \cup (G(\eta_M), \infty)$. Hence, there are single pre-images in the ranges $(0, \min\{G^{-1}(G(\eta_M))\})$ and $(\max\{G^{-1}(G(\eta_m))\}, 1]$. For $G(\eta_m) < G(\cdot) < G(\eta_M)$, there are three pre-images and for $G(\eta_m)$ and $G(\eta_M)$ there are exactly two due to the local minimum and maximum (see Fig. 5). Then, the smallest pre-image among them lies on $[\min\{G^{-1}(G(\eta_M))\}, \eta_m]$ whereas the largest lies on $[\eta_M, \max\{G^{-1}(G(\eta_m))\}]$. In conclusion, the overall *smallest* pre-images belong to

$$\begin{aligned} \mathcal{R}_1 & = (0, \min\{G^{-1}(G(\eta_M))\}) \\ & \quad \cup [\min\{G^{-1}(G(\eta_M))\}, \eta_m] = (0, \eta_m] \end{aligned} \quad (36)$$

whereas the *largest* pre-images belong to

$$\begin{aligned} \mathcal{R}_2 & = [\eta_M, \max\{G^{-1}(G(\eta_m))\}] \\ & \quad \cup [\max\{G^{-1}(G(\eta_m))\}, 1] = [\eta_M, 1]. \end{aligned}$$

In particular, $\mathcal{R}_{12} \triangleq (0, \min\{G^{-1}(G(\eta_M))\}) \subset \mathcal{R}_1$ and $\mathcal{R}_{22} \triangleq (\max\{G^{-1}(G(\eta_m))\}, 1] \subset \mathcal{R}_2$. By bounding the MMSE using (16) and replacing $u = \gamma/8$, we obtain the desired results.

REFERENCES

- [1] S. Verdú, *Multiuser Detection*. Cambridge, U.K.: Cambridge Univ. Press, 1998.
- [2] K. Halford and M. Brandt-Pearce, "New-user identification in a CDMA system," *IEEE Trans. Commun.*, vol. 46, no. 1, pp. 144–155, Jan. 1998.

- [3] T. Oskiper and H. V. Poor, "Online activity detection in a multiuser environment using the matrix CUSUM algorithm," *IEEE Trans. Inf. Theory*, vol. 48, no. 2, pp. 477–493, Feb. 2002.
- [4] B. Chen and L. Tong, "Traffic-aided multiuser detection for random-access CDMA networks," *IEEE Trans. Signal Process.*, vol. 49, no. 7, pp. 1570–1580, July 2001.
- [5] E. Biglieri, E. Grossi, M. Lops, and A. Tauste Campo, "Large-system analysis of a dynamic CDMA system under a Markovian input process," in *Proc. IEEE Int. Symp. Inf. Theory*, Toronto, Canada, Jul. 2008.
- [6] M. L. Honig and H. V. Poor, "Adaptive interference suppression in wireless communication systems," in *Wireless Communications: Signal Processing Perspectives*, H. V. Poor and G. W. Wornell, Eds. Englewood Cliffs, NJ: Prentice-Hall, 1998.
- [7] E. Biglieri and M. Lops, "Multiuser detection in a dynamic environment—Part I: User identification and data detection," *IEEE Trans. Inf. Theory*, vol. 53, no. 9, pp. 3158–3170, Sep. 2007.
- [8] T. Tanaka, "A statistical-mechanics approach to large-system analysis of CDMA multiuser detectors," *IEEE Trans. Inf. Theory*, vol. 48, no. 11, pp. 2888–2910, Nov. 2002.
- [9] D. Guo and S. Verdú, "Randomly spread CDMA: Asymptotics via statistical physics," *IEEE Trans. Inf. Theory*, vol. 51, no. 6, pp. 1983–2007, Jun. 2005.
- [10] D. Guo, Y. Wu, S. Shamai (Shitz), and S. Verdú, "Estimation in Gaussian noise: Properties of the minimum mean-square error," *IEEE Trans. Inf. Theory* vol. 57, no. 4, pp. 2371–2385, Apr. 2011.
- [11] H. Nishimori, *Statistical Physics of Spin Glasses and Information Processing: An Introduction*. Oxford, U.K.: Oxford Univ. Press, 2001.
- [12] D. Guo and T. Tanaka, "Generic multiuser detection and statistical physics," in *Advances in Multiuser Detection*, M. L. Honig, Ed. New York: Wiley, 2009.
- [13] M. Mézard and A. Montanari, *Information, Physics and Computation*. Oxford, U.K.: Oxford Univ. Press, 2009.
- [14] S. B. Korada and N. Macris, "Tight bounds on the capacity of binary input random CDMA Systems," *IEEE Trans. Inf. Theory* vol. 56, no. 11, pp. 5590–5613, Nov. 2010.
- [15] A. Tauste Campo and E. Biglieri, "Large-system analysis of static multiuser detection with an unknown number of users," in *Proc. IEEE Int. Workshop on Comp. Adv. Multi-Sens. Adapt. Process. (CAMSAP'07)*, Saint Thomas, US Virgin Islands, Dec. 2007.
- [16] A. Tauste Campo and E. Biglieri, "Asymptotic capacity of a static multiuser channel with an unknown number of users," in *Proc. IEEE Int. Symp. Wireless Pers. Mult. Commun. (WPMC'08)*, Sep. 2008.
- [17] A. Tauste Campo, A. Guillén i Fàbregas, and E. Biglieri, "High-SNR analysis of optimum detection with an unknown number of users," in *Proc. IEEE Inf. Theory Workshop*, Taormina, Italy, Oct. 2009.
- [18] E. Biglieri and M. Lops, "A new approach to multiuser detection in mobile transmission systems," in *Proc. IEEE Int. Symp. Wireless Pers. Mult. Commun. (WPMC'06)*, San Diego, CA, Sep. 2006.
- [19] D. Tse and S. Hanly, "Linear multiuser receivers: Effective interference, effective bandwidth, and user capacity," *IEEE Trans. Inf. Theory*, vol. 45, no. 2, pp. 641–657, Mar. 1999.
- [20] R. R. Müller, "Channel capacity and minimum probability of error in large dual antenna array systems with binary modulation," *IEEE Trans. Signal Process.*, vol. 51, no. 11, pp. 2821–2828, Nov. 2003.
- [21] R. S. Ellis, *Entropy, Large Deviations, and Statistical Mechanics*, ser. A Series of Comprehensive Studies in Mathematics. New York: Springer-Verlag, 1985, vol. 271.
- [22] V. Poor, *An Introduction to Signal Detection and Estimation*. New York: Springer-Verlag, 1988.
- [23] D. Tse and S. Verdú, "Optimum asymptotic multiuser efficiency of randomly spread CDMA," *IEEE Trans. Inf. Theory*, vol. 46, no. 11, pp. 2718–2722, Nov. 2000.
- [24] S. Verdú and S. Shamai(Shitz), "Spectral efficiency of CDMA with random spreading," *IEEE Trans. Inf. Theory*, vol. 45, no. 2, pp. 622–640, Mar. 1999.
- [25] M. Talagrand, *Spin Glasses: A Challenge for Mathematicians*. New York: Springer, 2003.
- [26] A. Montanari and D. Tse, "Analysis of belief propagation for non-linear problems: The example of CDMA (or: How to prove Tanaka's formula)," in *Proc. IEEE Inf. Theory Workshop*, Punta del Este, Uruguay, Mar. 2006.
- [27] S. B. Korada and A. Montanari, Applications of Lindeberg Principle in Communications and Statistical Learning [Online]. Available: <http://arxiv.org/abs/1004.0557>
- [28] D. Guo and C.-C. Wang, "Random sparse linear systems observed via arbitrary channels: A decoupling principle," in *Proc. IEEE Int. Symp. Inf. Theory*, Nice, France, Jun. 2007.
- [29] D. Guo, D. Baron, and S. Shamai (Shitz), "A single-letter characterization of optimal noisy compressed sensing," in *Proc. Allerton Conf. Commun., Contr. Comput.*, Oct. 2009.
- [30] A. Lozano, A. M. Tulino, and S. Verdú, "Optimum power allocation for parallel Gaussian channels with arbitrary input distributions," *IEEE Trans. Inf. Theory*, vol. 52, no. 7, pp. 3033–3051, Jul. 2006.
- [31] A. Tauste Campo and A. Guillén i Fàbregas, "Large system analysis of iterative multiuser joint decoding with an uncertain number of users," in *Proc. IEEE Int. Symp. Inf. Theory*, Austin, TX, Jun. 2010.

Adrià Tauste Campo (S'08) was born in Barcelona, Catalunya, Spain, in 1982. He received the Mathematics and Telecommunications Engineering degrees from the Universitat Politècnica de Catalunya, Barcelona, Spain, the European Master degree in information technologies from the Universitat Pompeu Fabra, Barcelona, in 2007, and the M.Sc. degree in electrical engineering from Stanford University, Stanford, CA, in 2009.

From September 2005 to March 2006, he carried out his final degree thesis at the Institute for Telecommunications Research, University of South Australia, Mawson Lakes, Australia. He is currently a Ph.D. student in the Department of Engineering and a member of Fitzwilliam College, University of Cambridge, Cambridge, U.K. From September 2006 to December 2007, he was a Research and Teaching Assistant with the Universitat Pompeu Fabra. Throughout the academic year 2009–2010, he was a Teaching Assistant and College Supervisor with the University of Cambridge, U.K., and from July to September 2010, he was an Intern with Telefonica Research Labs, Barcelona, Catalunya. He has held research visits with the Università di Cassino, Cassino, Italy, with the Universitat de les Illes Balears, Palma de Mallorca, Spain, and with the Universitat Pompeu Fabra, Barcelona.

Mr. Campo received a Graduate Fellowship from the Spanish savings bank "La Caixa" to study toward the M.Sc. degree in electrical engineering at Stanford University in 2007 and the Doctoral Training Account (DTA) from the Engineering and Physical Sciences Research Council (EPSRC), U.K., in 2007 to pursue the Ph.D. degree in engineering at the University of Cambridge. He is a Junior Member of the Isaac Newton Institute for Mathematical Sciences.

Albert Guillén i Fàbregas (S'01–M'05–SM'09) was born in Barcelona, Catalunya, Spain, in 1974. He received the Telecommunication Engineering degree and the Electronics Engineering degree from the Universitat Politècnica de Catalunya, and the Politecnico di Torino, Torino, Italy, respectively, in 1999, and the Ph.D. degree in communication systems from Ecole Polytechnique Fédérale de Lausanne (EPFL), Lausanne, Switzerland, in 2004.

From August 1998 to March 1999, he conducted his Final Research Project at the New Jersey Institute of Technology, Newark. He was with Telecom Italia Laboratories, Italy, from November 1999 to June 2000 and with the European Space Agency (ESA), Noordwijk, The Netherlands, from September 2000 to May 2001. During his doctoral studies, from 2001 to 2004, he was a Research and Teaching Assistant with the Institut Eurécom, Sophia-Antipolis, France. From June 2003 to July 2004, he was a Visiting Scholar with EPFL. From September 2004 to November 2006, he was a Research Fellow with the Institute for Telecommunications Research, University of South Australia, Mawson Lakes. Since 2007, he has been a Lecturer with the Department of Engineering, University of Cambridge, Cambridge, U.K., where he is also a Fellow of Trinity Hall. He has held visiting appointments at Centrum Wiskunde and Informatica, Amsterdam, The Netherlands; Ecole Nationale Supérieure des Télécommunications, Paris, France; Texas A&M University, Doha, Qatar; Universitat Pompeu Fabra, Barcelona; and the University of South Australia. His research interests are in communication theory, information theory, coding theory, digital modulation, and signal processing techniques with wireless applications.

Dr. i Fàbregas is currently an Editor of the IEEE TRANSACTIONS ON WIRELESS COMMUNICATIONS. He received the Starting Grant from the European Research Council, the Young Authors Award of the 2004 European Signal Processing Conference EUSIPCO 2004, Vienna, Austria, the 2004 Nokia Best Doctoral Thesis Award in Mobile Internet and 3rd Generation Mobile Solutions from the Spanish Institution of Telecommunications Engineers, and a pre-doctoral Research Fellowship of the Spanish Ministry of Education to join ESA. He is also a Senior Member of IEEE (Information Theory and Communications Societies).

Ezio Biglieri (M'73–SM'82–F'89–LF'10) was born in Aosta, Italy. He received the Dr. Engr. degree in 1967 in electrical engineering from the Politecnico di Torino, Torino, Italy.

He is presently an Adjunct Professor of Electrical Engineering at the University of California, Los Angeles (UCLA), and an honorary Professor with the Universitat Pompeu Fabra, Barcelona, Spain. Previously, he was a Professor with the University of Napoli, Napoli, Italy, with the Politecnico di Torino, and with UCLA. He has held visiting positions with the Department of System Science, UCLA; the Mathematical Research Center, Bell Laboratories, Murray Hill, NJ; Bell Laboratories, Holmdel, NJ; the Department of Electrical Engineering, UCLA; the Telecommunication Department of The Ecole Nationale Supérieure des Télécommunications, Paris, France; the University of Sydney, Australia; the Yokohama National University, Japan; the Electrical Engineering Department, Princeton University, Princeton, NJ; the University of South Australia,

Adelaide; the University of Melbourne, Australia; the Institute for Communications Engineering, Munich Institute of Technology, Germany; the Institute for Infocomm Research, National University of Singapore; the National Taiwan University, Taipei, Taiwan, R.O.C.; the University of Cambridge, U.K.; and ETH Zurich, Switzerland.

Prof. Biglieri was elected three times to the Board of Governors of the IEEE Information Theory Society, and he served as its President in 1999. He was the Editor-in-Chief of the IEEE TRANSACTIONS ON INFORMATION THEORY and is the Editor-in-Chief of the *Journal of Communications and Networks*. Among other honors, in 2000, he received the IEEE Third-Millennium Medal and the IEEE Donald G. Fink Prize Paper Award, in 2001 the IEEE Communications Society Edwin Howard Armstrong Achievement Award, and a Best Paper Award from WPMC01, Aalborg, Denmark, and in 2004, the *Journal of Communications and Networks* Best Paper Award.